

Growth of Crystalline Polyaminoborane through Catalytic Dehydrogenation of Ammonia Borane on FeB Nanoalloy

Teng He,^[a] Junhu Wang,^[a] Guotao Wu,^[a] Hyunjeong Kim,^[b] Thomas Proffen,^[b] Anan Wu,^[c] Wen Li,^[d] Tao Liu,^[e] Zhitao Xiong,^[a] Chengzhang Wu,^[a] Hailiang Chu,^[a] Jianping Guo,^[a] Tom Autrey,^[f] Tao Zhang,^[a] and Ping Chen*^[a]

Tremendous efforts have been devoted to the study of hydrides for hydrogen storage in the past decade.^[1,2] Ammonia borane (NH₃BH₃, AB) with a hydrogen content of 19.6 wt% has received significant attention.^[3–5] Methods to improve the kinetics of the step-wise dehydrogenation of AB are diverse including the uses of mesoporous frameworks,^[6] catalysts,^[7–16] and additives.^[17] It was reported that when dissolving AB in organic solvents hydrogen is released readily in the presence of transition-metal catalysts through the formation of a M··HBH₂NH₃ complex (where M = Ir, Ru, or Ni etc.).^[8–10] Lewis or Brønsted acids, on the other hand, react with AB in solution to form the initiating species (BH₂NH₃)⁺,^[11] which may have a similar function as [BH₂(NH₃)₂]⁺BH₄[−] (DADB) in the dehydrogenation of solid AB.^[17,18] However, comparatively little has been re-

ported on the catalytic dehydrogenation of AB in the solid form. Other important but less investigated aspects in the solid-state reaction are the characterizations of functional catalytic species and products from the step-wise dehydrogenation. Polyaminoborane (PAB) is commonly used as the solid component of the first-step dehydrogenation, which is essentially amorphous and likely composed of linear, branched or cyclic (NBH₄) oligomers and polymers.^[3,7,18] On the other hand, AB decomposition in the presence of an iridium pincer catalyst releases exactly one equivalent of hydrogen,^[9] and forms an insoluble PAB product that appears to have no branching and has some characteristics of the cyclic pentamer reported by Shore.^[19] Further investigations showed that crystalline PAB may be a more ordered linear oligomer and polymeric species.^[20] The chemical form of the PAB product relates to the reaction details and manifests the changes in thermodynamics and kinetics of the dehydrogenation. In this study, we present, for the first time, the development of a FeB nanoalloy of 2–5 nm in size for the catalytic dehydrogenation of solid AB. Our experimental results show that about 1.0 and 1.5 equiv H₂ can be released at 60 and 100 °C, respectively. In contrast to dehydrogenation of neat AB which yields non-crystalline products, the solid-state catalyzed dehydrogenation of AB yields crystalline PAB as a major product. Our simulation results indicate that AB may undergo intramolecular dehydrogenation in the presence of FeB and form monomeric NH₂BH₂. The polymerization of NH₂BH₂ provides either cyclized or linear formation of PAB. This is significantly different from the PAB observed in the thermal decomposition of AB.

FeCl₃ of 5.0 mol% was introduced to AB following the “co-precipitation” method developed recently.^[13] Transmission electron microscopy (TEM) observations show that the majority of the Fe-containing particles are 2–5 nm in size (Supporting Information, Figure S1). Temperature-programmed desorption/mass spectroscopy (TPD/MS) revealed that the Fe-doped AB sample started to evolve H₂ at about 55 °C, significantly lower than that of neat AB (Supporting

[a] T. He, Prof. J. Wang, Dr. G. Wu, Prof. Z. Xiong, Dr. C. Wu, Dr. H. Chu, J. Guo, Prof. T. Zhang, Prof. P. Chen
Dalian Institute of Chemical Physics
Chinese Academy of Sciences, 457# Zhongshan Road
116023 Dalian (China)
Fax: (+86) 411-84685940
E-mail: pchen@dicp.ac.cn

[b] Dr. H. Kim, Dr. T. Proffen
Lujan Neutron Scattering Center, Los Alamos National Laboratory
Los Alamos, New Mexico, 87545 (USA)

[c] Dr. A. Wu
State Key laboratory of Physical Chemical of Solid Surfaces
Xiamen University, YanWu Road, Xiamen, Fujian, 361005 (China)

[d] W. Li
Department of Physics, National University of Singapore
10 Kent Ridge Crescent, 117542 (Singapore)

[e] T. Liu
Institute for Synchrotron Radiation
Karlsruhe Institute of Technology, 76344 Karlsruhe (Germany)

[f] Dr. T. Autrey
Pacific Northwest National Laboratory
Richland, WA 99352 (USA)

Supporting information for this article is available on the WWW under <http://dx.doi.org/10.1002/chem.201001844>.

Information, Figure S2). Isothermal volumetric measurements at 60 °C show that little H₂ was released from neat AB upon holding the sample for 30 h (Figure 1). However,

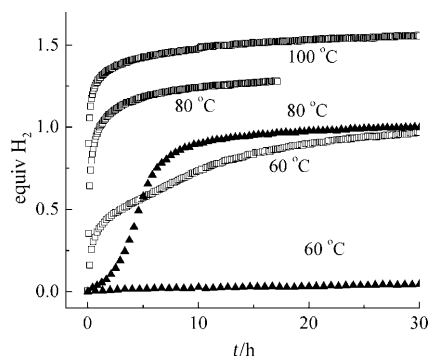


Figure 1. Volumetric release measurements on neat (▲) and 5.0 mol % Fe-doped (□) AB samples at different temperatures.

the Fe-doped AB evolved hydrogen immediately at 60 °C, without an observable induction period, showing a remarkable difference from the diammoniate of diborane (DADB) initiated sigmoidal dehydrogenation of solid AB.^[17,18] On heating the Fe-doped sample to 80 and 100 °C, more than 1.2 and 1.5 equiv H₂ can be released, which is greater than that of neat AB at these temperatures.^[17] In addition, the formation of side product borazine was significantly reduced, and the NH₃ yield is below the detection limit (10 ppm) in the Fe-doped AB sample (Supporting Information). Moreover, in contrast to neat AB, little foaming was observed upon heating the Fe-doped AB at temperatures up to 120 °C (Supporting Information, Figure S3). Note that slower but similar dehydrogenation behavior was observed from the sample with less FeCl₃ doping (i.e., 2 mol %).

X-ray diffraction (XRD) characterization shows that the post-dehydrogenated neat AB sample is essentially amorphous with a broad band centered at d of about 4.7 Å, while for the Fe-doped AB sample, a sharp diffraction peak at about 3.78 Å and weak peaks at 4.37, 2.86 and 2.19 Å are present (Supporting Information, Figure S4). These peaks matched very well with the diffractions of crystalline cyclopentaborazane (NH₂BH₂)₅, CPB,^[19,21] but may be a more ordered linear PAB.^[20] Fourier transform infrared (FTIR) spectroscopy of the post-dehydrogenated Fe-doped AB exhibits a similar pattern to crystalline PAB.^[19–21] Further evidence from the X-ray atomic pair distribution functions (PDFs)^[22] characterizations shows that the post-dehydrogenated Fe-doped AB sample has essentially similar patterns in both high and low- r regions as that of the PAB sample synthesized by the Ir-catalyzed decomposition of AB in THF,^[9,20] unlike PAB generated from thermal decomposition of solid AB, both PAB products, the one generated from Ir catalysis in solution, PAB_{Ir}, and the one generated from FeB catalysis in the solid state, PAB_{FeB}, show nice structural ordering in the detection range (4.0 nm). The PDFs determined B–N bond length of 1.56 Å is slightly

shorter than the calculated value,^[23] 1.60 Å, and is within the experimental error of the B–N bond length in cyclotriborazene, 1.57 Å.^[24] To our knowledge this is the first report on the formation of crystalline PAB through solid-state dehydrogenation of AB.

The selective growth of crystalline PAB_{FeB} reflects the catalyst-controlled dehydrogenation. ⁵⁷Fe Mössbauer spectroscopy investigations on the chemical state and local environment of Fe show that FeCl₃ was reduced by AB upon mixing (Supporting Information, Figure S6). A Fe species having an isomer shift of 0.19 mm s⁻¹, which is different from metallic Fe but similar to alloy of Fe and B, was formed.^[25] X-ray absorption spectroscopy (XAS) characterization shows that Fe in the alloy is in the reduced state and exhibits poor long distance ordering (see Supporting Information, Figure S7). We also noticed that after removing the crystalline PAB_{Ir} signal from the post-dehydrogenated sample, the PDFs pattern in the low- r regions (below 10 Å) resembles to that of the calculated pattern from the FeB structural model (Figure 2, III). A rapid decrease of the PDF peak height with increasing r (most of the signal fades out at 10 Å) reflects the absence of long-range structural order of FeB. PDFs peaks at about 2.10 and 2.57 Å are due to Fe–B and Fe–Fe pairs in FeB.

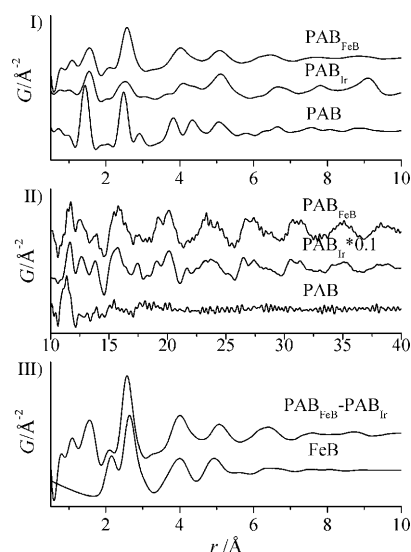


Figure 2. i) Low- and ii) high- r regions of the post-dehydrogenated Fe-doped AB (PAB_{FeB}), post-dehydrogenated Ir-catalyzed AB (PAB_{Ir}) and PAB from the thermal decomposition of AB; iii) the patterns of the calculated FeB and the post-dehydrogenated Fe-doped AB after removing PAB_{Ir} signal (PAB_{FeB}–PAB_{Ir}).

The characterization shown above strongly indicates the formation of FeB nanoalloy which may function as a catalyst in the dehydrogenation of solid AB. Analysis of the PAB_{FeB} by solid-state ¹¹B NMR analysis was inconclusive due to the presence of the paramagnetic iron species. From the Mössbauer isomer shift which mainly reflects the variation of electron density we can deduce that Fe in the FeB alloy has less electron density compare with metallic iron (0 mm s⁻¹)

since $\Delta R/R < 0$ for ^{57}Fe . Our simulation results on the Bader charges borne by Fe and B in FeB and Fe_2B also suggest that Fe is essentially in a reduced state but has certain positive charges (Supporting Information, Table S3). The partially positively charged Fe is likely to establish an interaction with the hydridic H in AB.

Gas-phase calculations were conducted (see Supporting Information) to gain preliminary insights to the interaction between FeB and AB. It should be noted that such molecular-level calculations only preliminary show the interaction of AB or aminoborane with FeB and the likely pathway of AB activation on FeB. The real path of solid-state reaction may be significantly different. As illustrated in Figure 3, AB and FeB form a stable complex **I**, with a BH...Fe bond length of 1.809 Å. The B–H and N–H bond lengths increase from 1.208 and 1.017 to 1.260 and 1.030 Å, respectively, showing the activation of both bonds through this interaction. Recent theoretical investigations indicate that concerted release of hydrogen from AB^[10,26,27] or amine boranes^[28,29] in molecular catalysis systems will lead to the formation of aminoborane. Similar dehydrogenation may take place in the AB/FeB system. Two transition states (**TS1** and **TS2**) with kinetic barriers of 7.3 and 14.9 kcal mol⁻¹, respectively, were identified. Compared with neat AB, the presence of FeB significantly reduces the kinetic barrier for the intramolecular dehydrogenation of AB. In comparison with **TS2**, the electrostatic interaction between the positively charged Fe and the hydridic H in AB further stabilizes the transition state and makes **TS1** (where one of the H of BH₃ moves towards Fe and forms a Fe–H bond) more preferable. After the concerted dehydrogenation, NH₂BH₂ is prone to form a complex (**II**) with FeB through BH...Fe coordination (Figure 3).

In a recent computational study, Rousseau et al. argued that a strong interaction between the BH and a Rh cluster catalyzed the decomposition of BH₃NH(CH₃)₂.^[30] NH₂BH₂ formed from the continuous catalytic dehydrogenation of

AB will polymerise into dimer, trimer, etc., in a chain growth manner. The polymerization may follow the Ziegler–Natta mechanism^[31] in the presence of FeB or the gas-phase polymerization proposed by Zimmerman et al.^[32] As there is a coordination between aminoborane and FeB indicated by the simulation results (Figure 3), we would propose a Ziegler–Natta-like polymerization in the present case. It is also worthy of noting that the highly linear and stereochemical pure polymer can be produced through the Ziegler–Natta polymerization due to the selective coordination of monomer to catalyst, which is significantly different from the less selective ion initiated (such as DADB) polymerization.

Although further investigations are needed, the growth of crystalline PAB through the proposed intramolecular dehydrogenation-chain growth mechanism should strongly depend on the composition/geometry of the catalyst and the match of the rates of crystal growth and dehydrogenation.

In summary, approximately 1.0 and 1.5 equiv H₂ was evolved from the FeB nanoalloy catalyzed AB at 60 and 100 °C, respectively, with depression of borazine and NH₃. Crystalline linear polyaminoborane was formed upon dehydrogenation, the growth of which may follow the dehydrogenation-chain growth mechanism.

Experimental Section

AB (Sigma–Aldrich, 97.0%), FeCl₃ (Sigma–Aldrich, 98.0%), and THF (99.8% J&K Chemical) were used without further purification. The preparation of AB doped with 5.0 mol% FeCl₃ followed the “co-precipitation” method described elsewhere.^[13] Noted that FeCl₃ is a precursor of the catalytic species, other Fe compounds such as FeCl₂ also work well. The catalyst loadings of 2, 5, 8 and 10% have been investigated. The 5%-doped system gave better performance in terms of H₂ capacity and reaction rate. All sample handlings were conducted in an MBraun 200 glove box filled with purified argon. XRD studies were carried out on a PANalytical X'pert diffractometer. A homemade TPD/MS system was employed to identify the gaseous products during sample decomposition. Homemade volumetric release apparatus was used to quantify the hydrogen released from samples. The gaseous products were introduced into a diluted sulphuric acid to detect the NH₃ concentration from the change of conductivity of the acid solution. Morphologies of samples were observed on a transmission electron microscope (FEI Tecnai G2). FTIR measurements were performed on a Varian 3100 unit in transmittance mode. The ^{57}Fe Mössbauer spectra were recorded using a Topologic 500 A spectrometer and a proportional counter at room temperature. $^{57}\text{Co}(\text{Rh})$ moving in a constant acceleration mode was used as radioactive source. Samples were protected by Ar during the Mössbauer measurements. Room temperature XAFS spectra were collected at BL14W1 beamline of Shanghai Synchrotron Radiation Facility. The X-ray RA-PDF experiment^[33] was conducted at the 11-ID-B beamline at the Advanced Photon Source at Argonne National Laboratory. An incident X-ray energy of 58.26 keV ($\lambda = 0.2128$ Å) was used. X-ray PDFs Raw data were processed using PDFgetX2 program.^[34] For structural modelling the program PDFgui^[35] was used.

Acknowledgements

We would like to acknowledge the financial supports from the Hundred Talents Project and Knowledge Innovation Program of CAS (KGCX2-YW-806 and KJCX2-YW-H21) 863 (2009AA05Z108) and 973

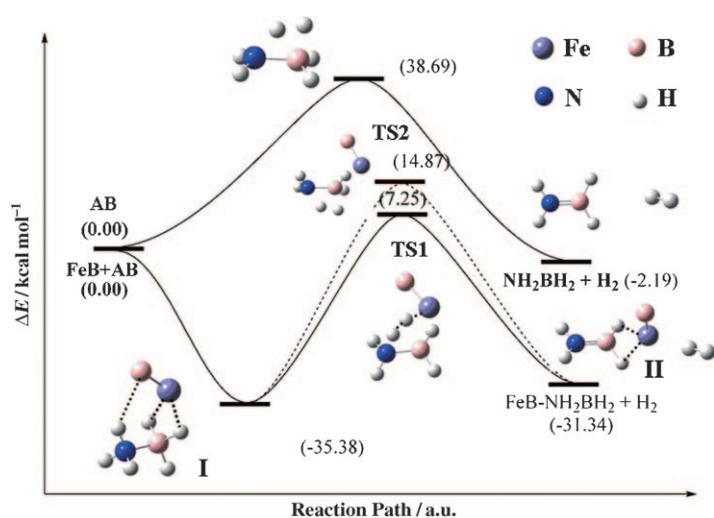


Figure 3. Simulation gas phase dehydrogenation mechanism of AB with or without FeB.

(2010CB631304) Project. XAFS experiments were performed in Shanghai Synchrotron Radiation Facility. Use of the Advanced Photon Source was supported by the US Department of Energy, Office of Science, Office of Basic Energy Sciences, under Contract No. DE-AC02-06CH11357. A.W. thanks NSFC(20703033). T.A. thanks US DoE Office of Basic Energy Sciences. We thank Drs. Heinekey and Goldberg (UW) for the generous gift of crystalline PAB from Ir-catalyzed AB.

Keywords: alloys • boranes • dehydrogenation • heterogeneous catalysis • nanoalloy

- [1] S. Orimo, Y. Nakamori, J. R. Eliseo, A. Züttel, C. M. Jensen, *Chem. Rev.* **2007**, *107*, 4111–4132.
- [2] P. Chen, M. Zhu, *Mater. Today* **2008**, *11*, 36–43.
- [3] G. Wolf, J. Baumann, F. Baitalow, F. P. Hoffmann, *Thermochim. Acta* **2000**, *343*, 19–25.
- [4] F. H. Stephens, V. Pons, R. T. Baker, *Dalton Trans.* **2007**, 2613–2626.
- [5] W. J. Shaw, J. C. Linehan, N. K. Szymczak, D. J. Heldebrant, C. Yonker, D. M. Camaioni, R. T. Baker, T. Autrey, *Angew. Chem.* **2008**, *120*, 7603–7606; *Angew. Chem. Int. Ed.* **2008**, *47*, 7493–7496.
- [6] A. Gutowska, L. Li, Y. Shin, C. M. Wang, X. S. Li, J. C. Linehan, R. S. Smith, B. D. Kay, B. Schmid, W. Shaw, M. Gutowski, T. Autrey, *Angew. Chem.* **2005**, *117*, 3644–3648; *Angew. Chem. Int. Ed.* **2005**, *44*, 3578–3582.
- [7] M. E. Bluhm, M. G. Bradley, R. Butterick, U. Kusari, L. G. Sneddon, *J. Am. Chem. Soc.* **2006**, *128*, 7748–7749.
- [8] R. J. Keaton, J. M. Blacquiere, R. T. Baker, *J. Am. Chem. Soc.* **2007**, *129*, 1844–1845.
- [9] M. C. Denney, V. Pons, T. J. Hebden, D. M. Heinekey, K. I. Goldberg, *J. Am. Chem. Soc.* **2006**, *128*, 12048–12049.
- [10] M. Käb, A. Friedrich, M. Drees, S. Schneider, *Angew. Chem.* **2009**, *121*, 922–924; *Angew. Chem. Int. Ed.* **2009**, *48*, 905–907.
- [11] F. H. Stephens, R. T. Baker, M. H. Matus, D. J. Grant, D. A. Dixon, *Angew. Chem.* **2007**, *119*, 760–763; *Angew. Chem. Int. Ed.* **2007**, *46*, 746–749.
- [12] D. W. Himmelberger, C. W. Yoon, M. E. Bluhm, P. J. Carroll, L. G. Sneddon, *J. Am. Chem. Soc.* **2009**, *131*, 14101–14110.
- [13] T. He, Z. Xiong, G. Wu, H. Chu, C. Wu, T. Zhang, P. Chen, *Chem. Mater.* **2009**, *21*, 2315–2318.
- [14] L. Li, X. Yao, C. Sun, A. Du, L. Cheng, Z. Zhu, C. Yu, J. Zou, S. C. Smith, P. Wang, H. Cheng, R. L. Cheng, R. L. Frost, G. Q. Lu, *Adv. Funct. Mater.* **2009**, *19*, 265–271.
- [15] R. P. Shrestha, H. V. K. Diyabalanage, T. A. Semelsberger, K. C. Ott, A. K. Burrell, *Int. J. Hydrogen Energy* **2009**, *34*, 2616–2621.
- [16] C. A. Jaska, K. Temple, A. J. Lough, I. Manners, *Chem. Commun.* **2001**, 962–963.
- [17] D. J. Heldebrant, A. Karkamkar, N. J. Hess, M. Bowden, S. Rassat, F. Zheng, K. Rappe, T. Autrey, *Chem. Mater.* **2008**, *20*, 5332–5336.
- [18] A. C. Stowe, W. J. Shaw, J. C. Linehan, B. Schmid, T. Autrey, *Phys. Chem. Chem. Phys.* **2007**, *9*, 1831–1836.
- [19] K. W. Bøddeker, S. G. Shore, R. K. Bunting, *J. Am. Chem. Soc.* **1966**, *88*, 4396–4401.
- [20] A. Staubitz, A. P. Soto, I. Manners, *Angew. Chem.* **2008**, *120*, 6308–6311.
- [21] http://www.hydrogen.energy.gov/pdfs/review06/st_4_heinekey.pdf.
- [22] Th. Proffen, H. Kim, *J. Mater. Chem.* **2009**, *19*, 5078–5088.
- [23] C. R. Miranda, G. Ceder, *J. Chem. Phys.* **2007**, *126*, 184703–184713.
- [24] P. W. R. Corfield, S. G. Shore, *J. Am. Chem. Soc.* **1973**, *95*, 1480–1487.
- [25] J. van Wonerghem, S. Mørup, C. J. W. Koch, S. W. Charles, S. Wells, *Nature* **1986**, *322*, 622–623.
- [26] A. Paul, C. B. Musgrave, *Angew. Chem.* **2007**, *119*, 8301–8304; *Angew. Chem. Int. Ed.* **2007**, *46*, 8153–8156.
- [27] X. Yang, M. B. Hall, *J. Am. Chem. Soc.* **2008**, *130*, 1798–1799.
- [28] Y. Luo, K. Ohno, *Organometallics* **2007**, *26*, 3597–3600.
- [29] Y. Kawano, M. Uruichi, M. Shimoi, S. Taki, T. Kawaguchi, T. Kaki-zawa, H. Ogino, *J. Am. Chem. Soc.* **2009**, *131*, 14946–14957.
- [30] R. Rousseau, G. K. Schenter, J. L. Fulton, J. C. Linehan, M. H. Engelhard, T. Autrey, *J. Am. Chem. Soc.* **2009**, *131*, 10516–10524.
- [31] E. J. Arlman, *J. Catal.* **1964**, *3*, 89–98.
- [32] P. M. Zimmerman, A. Paul, Z. Zhang, C. B. Musgrave, *Inorg. Chem.* **2009**, *48*, 1069–1081.
- [33] P. J. Chupas, X. Qiu, J. C. Hanson, P. L. Lee, C. P. Grey, S. J. L. Billinge, *J. Appl. Crystallogr.* **2003**, *36*, 1342–1347.
- [34] X. Qiu, J. W. Thompson, S. J. L. Billinge, *J. Appl. Crystallogr.* **2004**, *37*, 678.
- [35] C. L. Farrow, P. Juhas, J. W. Liu, D. Bryndin, E. S. Božin, J. Bloch, Th. Proffen, S. J. L. Billinge, *J. Phys. Condens. Matter* **2007**, *19*, 335219–335225.

Received: June 30, 2010
Published online: October 11, 2010